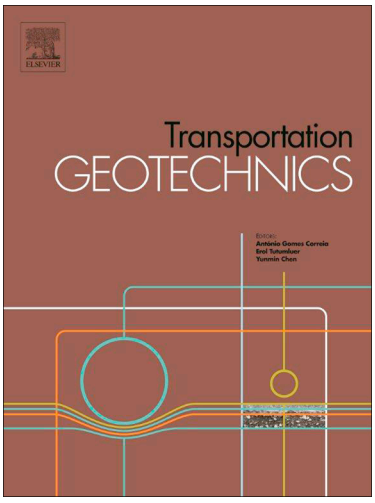

Train loading effects in railway geotechnical engineering: ground response, analysis, measurement and interpretation

William Powrie, Louis Le Pen, David Milne, David Thompson

PII: S2214-3912(19)30206-5
DOI: https://doi.org/10.1016/j.trgeo.2019.100261
Article Number: 100261
Reference: TRGEO 100261

To appear in: *Transportation Geotechnics*

Received Date: 24 May 2019
Revised Date: 10 July 2019
Accepted Date: 14 July 2019

Please cite this article as: W. Powrie, L. Le Pen, D. Milne, D. Thompson, Train loading effects in railway geotechnical engineering: ground response, analysis, measurement and interpretation, *Transportation Geotechnics* (2019), doi: https://doi.org/10.1016/j.trgeo.2019.100261

Train loading effects in railway geotechnical engineering: ground response, analysis, measurement and interpretation

William Powrie, Louis Le Pen, David Milne, David Thompson (University of Southampton, UK)

ABSTRACT

The engineered support system and the natural ground below a railway track are subjected to potentially many millions of cycles involving the application of moving loads. Thus dynamic, inertial and rate of loading effects, which can reasonably be neglected in many geotechnical applications, may need to be considered – along with the associated response of the geomaterials. Differences in the spacing of wheels along a train (e.g. between axles on the same bogie, and between bogies on the same or adjoining carriages) result in a spectrum of loading frequencies, rather than a single representative value. The dominant loading frequencies within the spectrum may vary with depth or distance from the track, and may be of differing importance in relation to different phenomena. All this has implications for the measurement and interpretation of data, and for the acceptability of simplifications made in testing and analysing the response of the ground and geotechnical structures. This paper summarises and discusses recent developments and thinking in these areas, in relation to the performance of ballasted railway track subjected to moving loads from trains travelling at a range of speeds.

INTRODUCTION

Trains apply repeated, moving loads of differing magnitudes through the superstructure (rails and sleepers) onto the substructure (ballast and subgrade soils) supporting a railway track. The frequencies of these loads depend on the train speed, axle spacing, and unevenness of the wheel / rail interface. Thus dynamic, inertial and rate of loading effects and the associated response of the material, which can all reasonably be neglected in many geotechnical applications, must at least be considered. They may be of relevance, both in analysing the real behaviour of railway track foundations and in specifying appropriate loading sequences in laboratory rig and element tests in which it is attempted to simulate spatial and temporal patterns of real train loading.

Loading associated with train passage is often described as “dynamic”. However, there is potential ambiguity in the use of the adjective “dynamic” in this context. The *loading* applied by trains is certainly dynamic; both in the sense that the train is moving so that loading at a given location varies with time, and because the vertical load experienced by the track and subgrade deviates from the (static) train axle load (due to the weight of the vehicle and its contents), as a result of additional forces associated with train movement. These additional forces arise primarily from dynamic excitation of the unsprung mass of the vehicle (e.g. the wheelsets) and the track system due to changes in trackbed stiffness and unevenness at the wheel / rail interface (which may be either random or associated with specific faults or features).

Conversely, at or in the trackbed, the *response* of well performing, plain line track and the ground supporting it can often be treated as quasi-static in the sense that inertial effects associated with the acceleration of the track and the ground are not significant for track bed movement at normal train speeds, even though the load is dynamic in the sense defined above (Timoshenko and Langer 1932

Higher frequency excitation resulting from unevenness or roughness at the wheel/rail interface is responsible for noise and vibration (Thompson 2009). This higher frequency excitation generates waves that propagate away from the track as ground-borne vibration, generally in the frequency range 10-250 Hz (Sheng et al 2003, Auersch 2005, Thompson 2009, Triepaischajonsak et al 2011, Grassie 2012, Alves Costa et al 2012, Connolly et al 2014, Lombaert et al 2015). However, the strains associated with ground-borne vibration from high frequency excitation are usually small compared with those associated with lower frequencies. Thus the primary concern from high frequency excitation is generally its impact on humans living nearby, and while this is important it is not usually relevant to the long term performance of the trackbed.

Wave propagation through the ground only becomes important for railway track displacement when the train speed v approaches the Rayleigh wave speed of the track / ground system, which is often referred to as the critical velocity (v_{crit}). Beyond a threshold

train speed, ground displacements can start to increase dramatically (e.g. Madshus and Kaynia 2000); dynamic (inertial) effects may then need to be taken into account in assessing the soil response. Non-linearity of the soil stiffness may also have an effect (Alves Costa et al 2010, Shih et al 2017). A train speed v of $0.7v_{crit}$ is often taken as the threshold at which these effects begin to become important (Dieterman and Metrikine 1996, 1997; Mezher et al 2016). Critical velocity effects are usually only a concern where soils are particularly soft and / or train speeds are particularly high, but in those circumstances they require specific attention.

Provided v is less than at least $0.7v_{crit}$, the major trackbed movements will be dominated by the relatively low frequency loading associated with the passing of the train vehicles, bogies and axles. For well-performing track, the velocities and accelerations associated with this loading are unlikely to be large enough to affect the material response, which remains essentially static and not significantly affected by variations in frequency within the low frequency range.

Low frequency loading from trains causes differential settlement along the track and an associated deterioration in track geometry with increasing numbers of train passes. If the geometry deteriorates excessively, ride comfort may reduce and ultimately the track may become unsafe for train operation. Maintenance – usually by tamping – is carried out before the geometry quality deteriorates too much. Maintenance is costly, not only in itself but also in the disruption caused to normal operations; hence there is a financial incentive to reduce the need for it.

To improve the understanding of the mechanisms of track differential settlement and to develop trackbed specifications for reduced maintenance, laboratory experiments have been carried out to investigate the response of ballast and soils to many applications of cyclic loading (e.g. Shenton 1984, Sato 1995, Indraratna et al 1998, Abadi et al 2016). In such tests it is common to simplify the loading to a single sinusoidal frequency. Some researchers state that this is not intended to represent the exact pattern of loading imposed in reality, but offers a reproducible benchmark test for comparing different designs of track support system. Others take the passing frequencies corresponding to the distances between adjacent axles or bogies for a particular train and speed as representative of field conditions. However, axle and bogie passing frequencies are not the same as the spectra of the train loading or the trackbed response, both of which result from a combination of train and track characteristics and cannot conveniently be represented as a single characteristic frequency. It is also usual to neglect entirely the higher frequency components that result primarily from wheel / rail unevenness.

The foregoing arguments lead to the conclusion that, in most circumstances, track bed performance will depend most significantly on low frequency loading. However, the magnitude, duration and combined effects of the spectrum of loading frequencies present

will all have an influence, as will the behaviour of the materials comprising the trackbed. This paper explores how loading frequencies, magnitudes and durations of displacements, velocities and accelerations impact on track performance with reference to the response of geotechnical materials to repeated loading; and how the spectra experienced by a ballast or soil element below the track relate to the spectrum of loading associated with train passage.

RESPONSE OF GEOTECHNICAL MATERIALS TO CYCLIC LOADING

Although the literature (e.g. Collins and Boulbibane 2000, Suiker and de Borst 2003, Qian et al 2016) is not entirely consistent in terms of either the descriptions of phenomena or terminology, broadly speaking an engineering material subjected to repeated cycles of loading may respond in one of five idealised ways:

1. Elastic. Strains are proportional to the current applied stress, and are fully reversible in that all of the strain experienced as a load is applied is recovered when the load is removed. There is no cumulative or adverse effect of repeated loading within the elastic loading range.
2. Elastic shakedown. Plastic (residual) strains develop during each of the initial load cycles. The amount of plastic strain decreases with each cycle until a stable elastic state is reached, after which the in-cycle strains are recoverable and no further plastic strain accumulates.
3. Plastic shakedown. Plastic (residual) strains develop during each of the initial load cycles. The amount of plastic strain decreases with each cycle until a stable state is reached, such that while there is some hysteresis over a cycle no further plastic strain accumulates.
4. Cyclic creep: plastic strains develop with every cycle, but at an ever-decreasing rate.
5. Ratcheting: plastic strains develop with every cycle, but at an increasing rate such that at some point the strains start to accumulate rapidly and failure or collapse ensues.

The first two of these responses apply to soils in only an approximate or idealised sense. The last three are illustrated by the results of cyclic hollow cylinder tests on a simulated railway subgrade material in Figure 1 (Mamou et al 2017). These tests simulate the effects of principal stress rotation in the subgrade below a ballasted railway track: the deviator stress was cycled between 0 and 30 kPa and the cyclic shear stress $\tau_{\theta z}$ was increased in stages from $\pm$8.5 kPa to $\pm$29.5 kPa, with a phase lag of 90°. Perhaps as a result of the magnitude of the initial stress cycle, no purely elastic phase was observed and shakedown was always plastic (i.e., the stress cycles always exhibited some hysteresis).

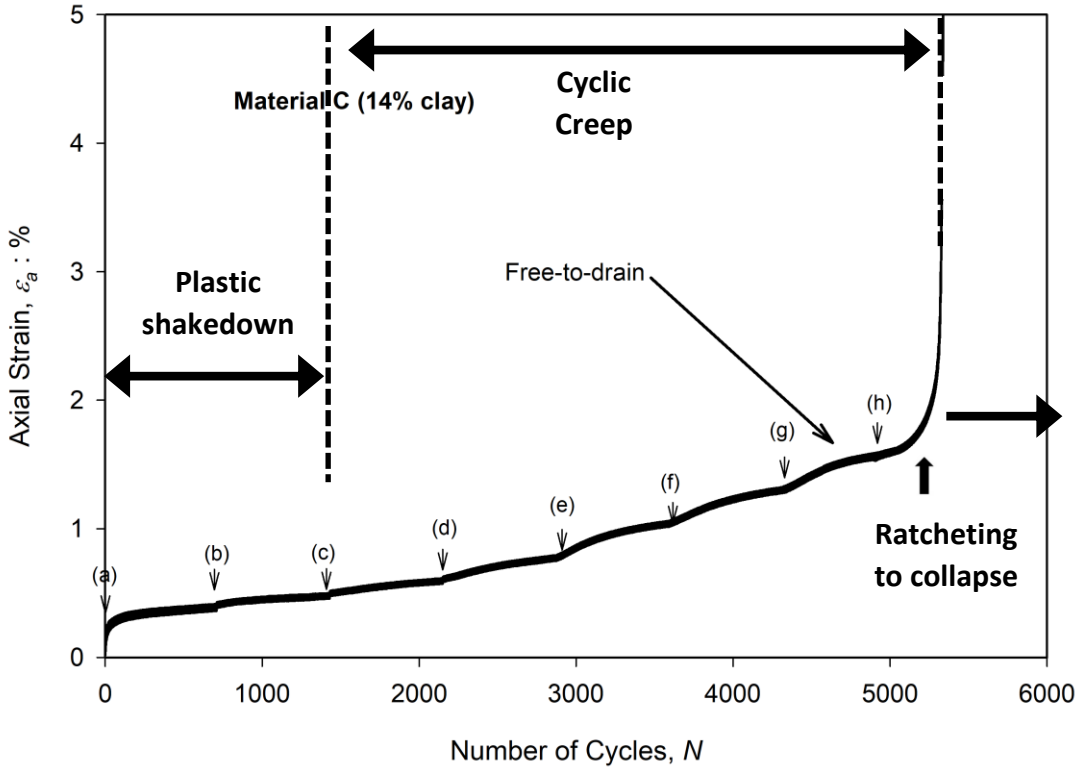

Figure 1: Plastic shakedown, cyclic creep and ratcheting to collapse of a simulated railway sub-base material in cyclic hollow cylinder tests with principal stress rotation (Mamou et al, 2017). The letters (a), (b), (c) etc indicate an increase in the magnitude of the cyclic shear stress, which was increased in steps of ±3 kPa from ±8.5 kPa to ±29.5 kPa

In materials terms the reasons for this behaviour are that

- in an initial loading cycle, a granular material undergoes both (i) irrecoverable (plastic) deformation due to inter-grain slip as the soil skeleton adjusts to carry the increase in load, and (ii) recoverable deformation due to the elastic distortion (without slip) of individual grains under load;
- with increasing numbers of load cycles, damage to the grain surface caused by abrasion (Figure 2), or even breakage of the grains, may cause an ongoing reduction in resistance to inter-grain movement, resulting in the gradual accumulation of plastic strains.

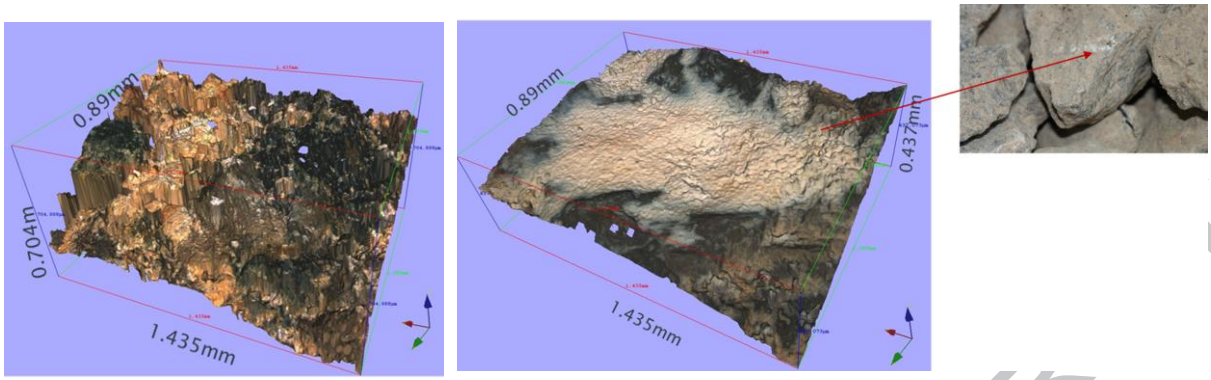

Figure 2: Ballast grain to grain contact patch surface roughness (a) initially; (b) after 3 million loading cycles in the Southampton Railway testing Facility (photographs: Dr B M Madhusudhan)

NON-MATERIAL FACTORS

The extent to which the material is constrained laterally is also important. For a railway on a firm subgrade, much of the continuing vertical settlement occurs as a result of the lateral spreading of unconfined ballast heaped in a steep "shoulder" to the side of the track (Figure 3). Thus the apparent plastic "cyclic creep" may well be at least in part a function of geometry, lateral restraint or stress ratio, rather than degradation of the material *per se*.

Figure 3: Typical steep ballast "shoulder" on a UK railway

This is illustrated by the results of sleeper rig tests reported by Abadi et al (2018). Plastic settlements over 3 million cycles of vertical load were reduced significantly by changing the slope of the ballast shoulder from 1:1 to 1:2 (Figure 4). Analysis of photographic images of the shoulder slope face demonstrated that this was associated with a substantially reduced movement of ballast grains down the shoulder slope (Abadi et al 2018). Significant reduction in the rate of settlement when the ballast bed is constrained laterally was also reported by Lackenby et al (2007).

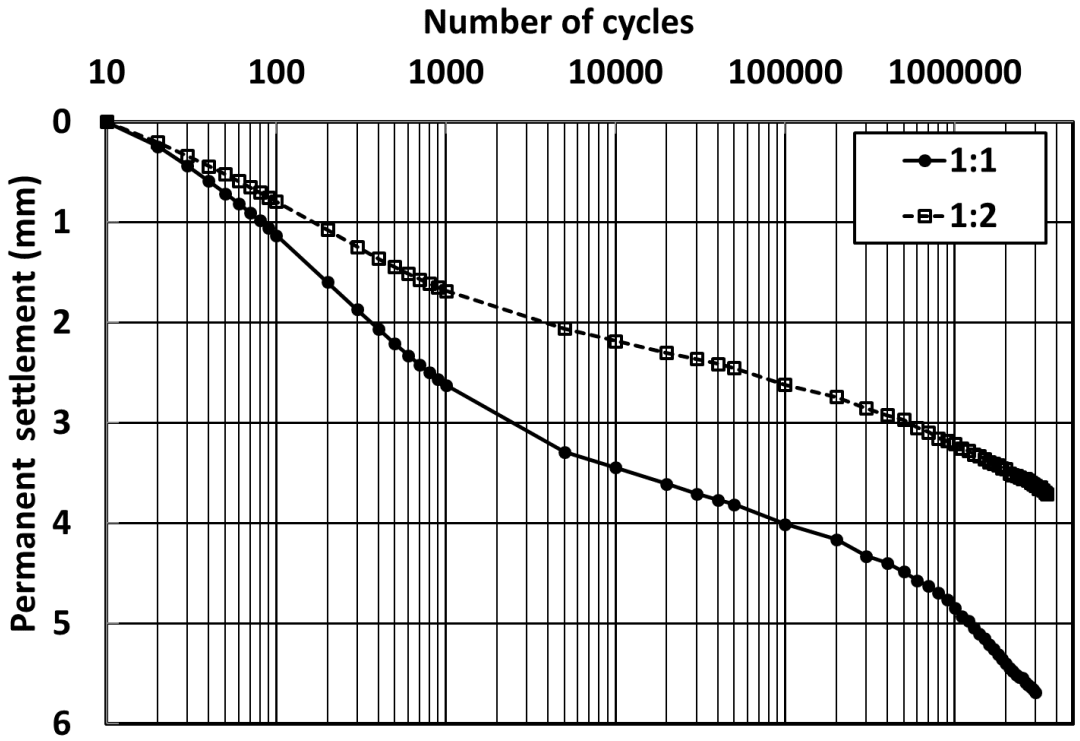

Figure 4: Permanent settlement vs number of cycles of a 20 tonne equivalent axle load applied at 3 Hz: shoulder slope 1:1 and 1:2 (redrawn from Abadi et al 2018)

DYNAMIC RESPONSE EFFECTS

As the amplitude and / or frequency of vibration increase, there will come a point at which the associated grain accelerations can no longer be considered negligible and the response of the material will change from quasi-static to dynamic. For simple harmonic motion of amplitude A and range 0 to $2A$, the displacement x takes the form $x = A.[1 - \sin\omega t]$ where ω is the circular frequency (= $2\pi \times$ the frequency, f in Hz). The maximum acceleration a_{max} is

$$a_{max} = \omega^2 A = \omega^2 .F/2k \qquad (1)$$

for a maximum applied load F and an equivalent spring stiffness k (so that $F = k.2A$). Thus the maximum acceleration depends not only on the frequency, but also on the amplitude of vibration or the load and the stiffness.

Sun et al (2018) report data from cyclic triaxial tests carried out at cell pressures of 10, 30 and 60 kPa, in which specimens of railway ballast were subjected to 20 000 cycles of deviatoric stress q of 0 to 230 kPa, at frequencies increasing in increments of 6 Hz from 6 to 30 Hz. Maximum ballast accelerations may be deduced using Equation 1 from the resilient moduli (effective stiffness) reported at the start of each stage by Sun et al (2018), the sample height, the frequency of loading and the deviatoric stress range (= F) of 230 kPa.

These are given in Table 1, which is shaded to distinguish stable (shakedown) from less stable (cyclic creep) regimes.

Cell pressure	Test frequency and acceleration in terms of *g* for given cell pressure				
	6 Hz	12 Hz	18 Hz	24 Hz	30 Hz
10 kPa	0.05g	0.18g	0.45g	1.8g	2.5g
30 kPa	0.06g	0.24g	0.43g	1.2g	2.5g
60 kPa	0.39g	0.20g	0.36g	0.75g	1.8g

Table 1: Maximum ballast accelerations (as a proportion or multiple of g) leading to plastic shakedown or cyclic creep in cyclic triaxial tests carried out by Sun et al (2018), calculated according to Equation (1) assuming simple harmonic motion. Shaded cells indicate cyclic creep, and unshaded cells plastic shakedown

The threshold maximum acceleration distinguishing shakedown from cyclic creep increases with confining stress, but even at the lowest cell pressure of 10 kPa approached 0.45g .For comparison, Eurocode EN 1990:2002+A1:2005 (BSI, 2010) stipulates a maximum vertical acceleration of 0.35g at frequencies of typically up to 30 Hz for ballast on railway bridge decks.

Sato (1995) related track degradation to train and track characteristics using a relatively simple empirical equation that included a term for ballast acceleration, which implied a rate of track geometry degradation proportional to $1/\sqrt{k}$ – that is, the smaller the trackbed stiffness the more significant the effect of acceleration. This is qualitatively consistent with Equation 1.

PRINCIPAL STRESS ROTATION

Below the track, the changes in stress to which a soil element is subjected during train passage initially become more complex with increasing depth. Specifically, the soil element begins to experience the effect of an oncoming train from some distance away, as a shear stress that gradually increases, falls to pass through zero when the train is immediately above, and then increases in the opposite sense before returning to zero as the train recedes. This is in addition to an increase in vertical stress, which peaks as the train passes directly above and then decreases monotonically back to zero as the train recedes. The shear stress is 90° out of phase with the normal stress increment, and the two together result in a rotation of the direction of major principal effective stress as the train approaches, passes and recedes. This is shown in Figure 5 and discussed in detail by Brown (1996), Gräbe and Clayton (2009), and Mamou et al (2017, 2018). Principal stress rotation does not occur immediately below the sleepers (because the horizontal distance at which the load starts to be felt is too small), while at great depths the whole loading regime

becomes insignificant. Thus principal stress rotation is most likely to be important in the subgrade layers immediately below the ballast.

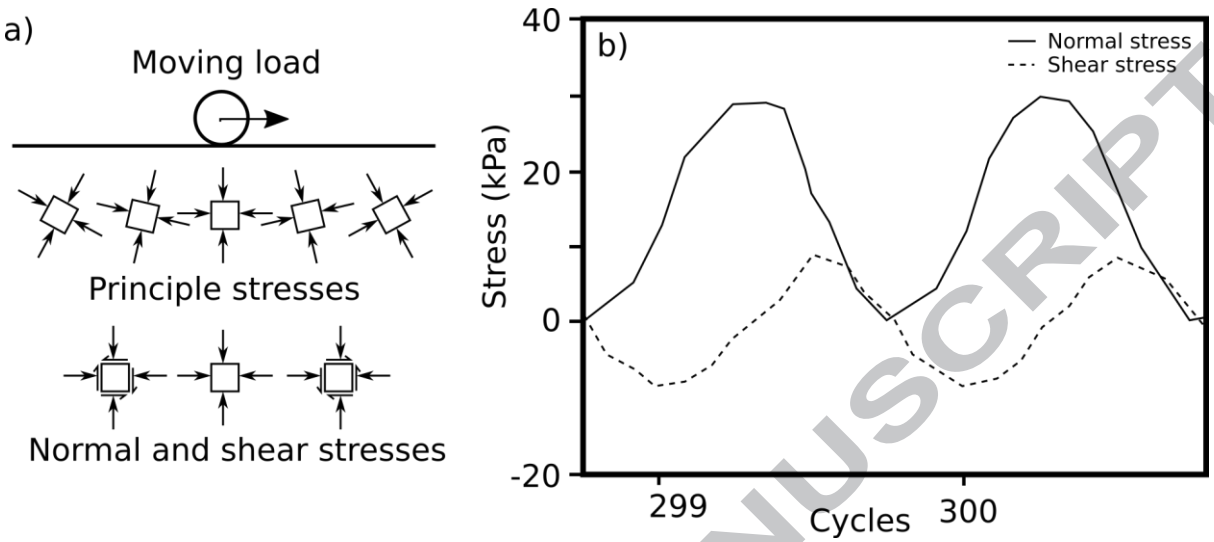

Figure 5 a) Principle stress rotation beneath a moving load and b) typical axial and shear stress cycles in a testing apparatus, redrawn from Brown (1996) and Mamou et al (2018)

Principal stress rotation was demonstrated in 3D finite element analyses presented by Powrie et al (2007) at depths between 0.3 m and at least 1.2 m below the sleeper soffit, depending on the initial major principal effective stress direction or in situ lateral earth pressure coefficient K_0. As demonstrated by Gräbe and Clayton (2009), some materials may exhibit less stable behaviour when subjected to load cycles that include principal stress rotation than under uniaxial cyclic loading. This is important at a range of depths of 0.3 m to perhaps 3 m below the sleeper soffit – that is, deep enough for the ground to experience principal stress rotation but not so deep that the stresses have substantially attenuated.

DRAINAGE DURING OR BETWEEN LOADING

In high permeability soils (gravels and clean sands), loading is likely to be in geotechnical terms fully drained, such that no excess (non-equilibrium) pore water pressures are generated. In low permeability soils, at least some of the applied load will be carried by an increase in pore water pressure, so as to maintain constant effective stress comparable with undrained or constant volume conditions. The effect of passing trains on pore water pressures or groundwater levels was reported by Jacob (1939).

In soils of intermediate permeability, some drainage and dissipation of the excess pore water pressures induced by train loading may occur during or between train passages. In this case, the frequency of loading relative to the timescale for excess pore water pressure dissipation may be important. The latter depends on the consolidation coefficient of the soil ($c_v = k.E'_o/\gamma_w$, where k is the permeability, E'_o is the one-dimensional modulus and γ_w is the unit weight of water) and the drainage path length d. Ideally, the loading frequency f and

the maximum drainage path length d in a laboratory test should be chosen to give equality of the dimensionless group $c_v/f.d^2$ (which governs consolidation time) between the laboratory and the field.

For the purpose of assessing drainage, the relevant loading event is probably the passage of a train, with the period between trains offering an opportunity for residual excess pore water pressure dissipation. The field drainage path length is given by the maximum depth of soil at which significant loading is experienced, say 3 m to 4 m (e.g. Powrie et al 2007). For a laboratory specimen 0.2 m high with one way drainage, equality of $c_v/f.d^2$ requires the actual frequency of train passage to be increased by the ratio of the square of the drainage path lengths; that is, a factor of (3^2 m^2 ÷ 0.02^2 m^2) to (4^2 m^2 ÷ 0.02^2 m^2), or 225 to 400. A train passing frequency of 10 to 20 trains per hour would therefore correspond to a loading frequency in a triaxial test of 0.625 to 2.22 Hz. This may not be feasible with standard apparatus and other considerations might militate against the approach: control of specimen drainage during load cycling might then offer an alternative option.

EFFECT OF TRAIN SPEED

Increasing train speed leads to an increase and greater variability in wheel loads, hence trackbed and subgrade deflections. This is because dynamic loads, arising primarily from accelerations of components of the vehicle, become more significant as train speeds increase. Accelerations of unsprung masses (the wheels and axles) occur as a result of short wavelength wheel / rail roughness. Accelerations of both sprung and unsprung masses over longer wavelengths also occur, associated with variations in the track support system stiffness, the discrete nature of sleeper supports and longer wavelength track geometry irregularities (Jenkins et al., 1974, Iwnicki, 2006). In trackbed design, dynamic vertical loads are traditionally taken into account by means of a dynamic load amplification factor (DAF) (e.g. Li & Selig 1998, AREA 1996). Dynamic load increments may be both positive or negative, hence the DAF gives the maximum load the trackbed should be designed to resist. Discussions of the use and theoretical basis of DAFs, a comparison with field measurements and numerical analyses, and some observations on their accuracy and their theoretical basis are given by Esveld 2001, Van Dyk et al 2017, Priest & Powrie 2009, Yang et al 2009, and Lord et al 1999 respectively.

Where subgrades are soft, the train speed can approach the velocity of surface (Rayleigh) waves in the underlying ground and resonance effects can lead to large increases in track displacement (Timoshenko 1927; Krylov 1995, 1996; Woldringh & New 1999; Madshus & Kaynia 2000; Mezher et al., 2016). Finite element analyses by Yang et al (2009) indicated displacements and subgrade stresses at a train speed of 0.1 × the velocity (v_c) of Rayleigh waves in the subsoil that were almost identical to those in a static analysis. The maximum track displacements increased gradually with increasing train speed, until the Rayleigh wave velocity v_c was approached when the increase in displacements was dramatic. Vertical and longitudinal-plane shear stresses in the subgrade increased roughly in proportion to the

train speed as the train speed was increased from 0.1 v_c to v_c . At a train speed of v_c, the shear stress was about 80% greater and the vertical stress about 20% greater than calculated in a static analysis.

The assessment and significance of dynamic load or displacement amplification and resonance phenomena depend on a wide variety of factors including the make-up of the subgrade, the train type and the track form, and are still a subject of some uncertainty. A detailed discussion of these phenomena is outside the scope of this paper.

ANALYSIS OF TRAIN LOADING

The train applies loads to the track through the wheels; axles are usually paired in bogies at both ends of or between each car. Thus as a train passes, the track at a given location will experience a repeated pattern of two or four axle loads in rapid succession, with a longer gap as the car body passes. There will then be a period with no load before the next train passes.

The most significant track movements arise from the response of the track and trackbed under the weight of the train, and can be assessed using the beam-on-elastic-foundation (BOEF) model (e.g. Timoshenko 1927, Raymond et al 1985, Esveld 2001; Figure 6).

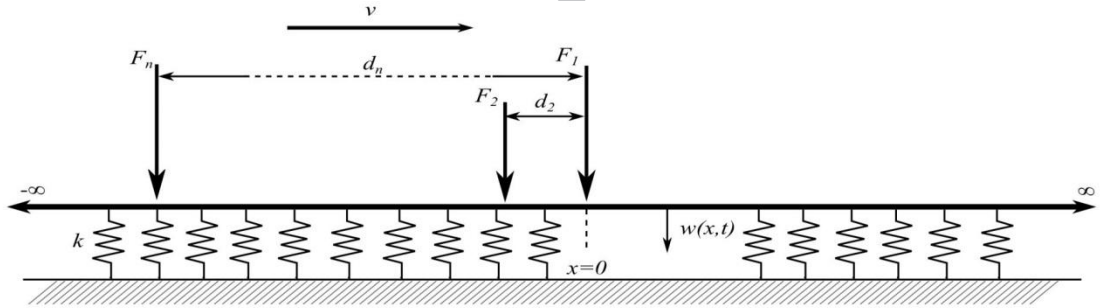

Figure 6 Beam on an elastic foundation (BOEF) conceptual model for railway track

The displacement at the rail *w* in response to a single load *p* (both, in principle, functions of horizontal distance *x* and time *t*) may be related through the equation of equilibrium for the beam. Neglecting inertial effects,

$$EI\frac{\partial^4 w(x,t)}{\partial x^4} + kw(x,t) = p(x,t) \qquad (2)$$

where *EI* is the bending stiffness of the track (which for ballasted track can be assumed to come entirely from the rails) and *k* is the track support system modulus (defined as the line load, for example in MN/m^2, needed to cause a unit deflection, to which the ballast, subgrade, natural ground, railpads and under sleeper pads all contribute).

Solving Equation (2) for the displacement at $x = 0$ for a single, unit point load moving at a velocity v gives

$$w(t) = s(t) = \frac{1}{2kL} e^{-\frac{v|t|}{L}} \left(\cos\left(\frac{v|t|}{L}\right) + \sin\left(\frac{v|t|}{L}\right) \right) \quad (3)$$

Equation (3) also describes the deflected shape of the track, and is therefore also known as the "shape function", $s(t)$.

For a succession of loads all moving at the same velocity v, where the ordinate of the nth load is d_n, the load function is:

$$p(x,t) = \sum_{n=1}^{N} F_n \left(\delta(x - d_n - vt) \right) \quad (4)$$

and the solution to Equation (2) for the deflection w at $x = 0$ and time t becomes

$$w(t) = \sum_{n=1}^{N} \frac{F_n}{2kL} e^{-\frac{|vt-d_n|}{L}} \left(\cos\left(\frac{|vt-d_n|}{L}\right) + \sin\left(\frac{|vt-d_n|}{L}\right) \right) \quad (5)$$

Equation (5) is plotted for a series of four vehicles of a Hitachi Class 395 "Javelin" type train, on a single rail for three different values of track support system modulus k in Figure 7; train and track properties are shown in Table 2. As the track support system stiffness is reduced, the displacement under each wheel and the lateral spread of the displacement bowl increase, while the proportional recovery of displacement between axles or bogies reduces.

Train properties	Bogie spacing	14.2 m
	Axle spacing	2.6 m
	Wheel load (F_N)	54.2 kN
Rail properties (60 E1 type)	E	205 GPa
	I	3038 cm^4

Table 2: Train and rail properties used in example calculations

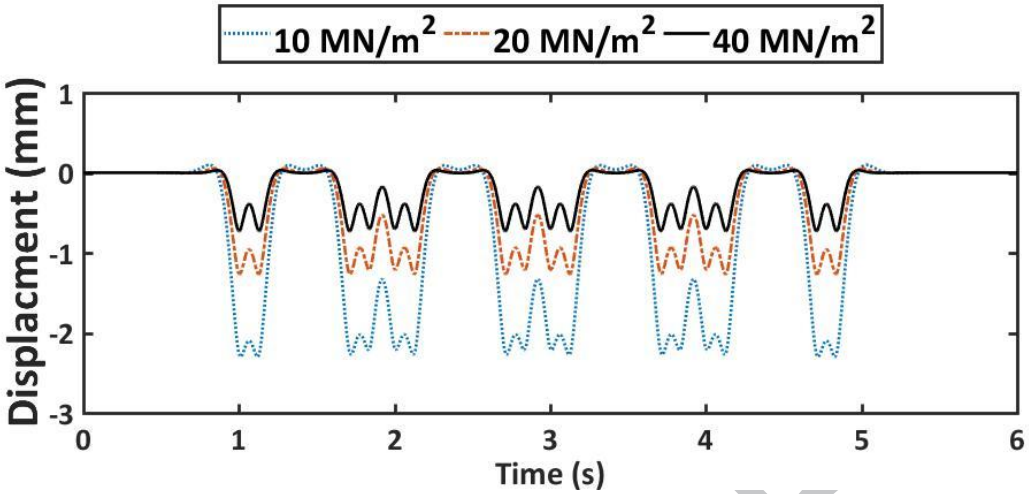

Figure 7: BOEF analysis results for axle loadings corresponding to a four-car Javelin train travelling at a speed v = 20 m/s; and varying track support system moduli

The corresponding velocities and accelerations, determined by differentiating the displacements numerically at a sampling rate (in effect, the frequency of data point acquisition) of 500 Hz, are shown in Figure 8 for a train speed of 20 m/s (72 km/h). This is equivalent to measuring an actual trace for a 20 m/s train at 500 Hz, and gives results that are quantitatively indistinguishable from those that would be calculated using a theoretically differentiated closed form solution for all normal operating train speeds.

Magnitudes of directly measured or numerically calculated accelerations inferred from displacement (or velocity) measurements depend on the sampling rate of the native measurement data as well as on the train speed. This has implications for the rate at which displacements, velocities and accelerations should be measured, signal conditioning and the application of standards providing limiting values (e.g. BSI 2010). As the sampling rate of a true instantaneous displacement is reduced below a certain sampling rate threshold (approximately 100 times the vehicle passing frequency, neglecting rail unevenness / roughness), the numerically inferred accelerations reduce – even though the peaks and troughs of the displacement trace largely remain. This is because of smoothing as the acceleration (the gradient of the velocity trace) is determined over increasing time intervals.

As the train speed increases, the magnitudes of displacements remain unaltered according to the BOEF model but the velocities and accelerations increase in proportion to v and v^2 respectively. Figure 9 shows that the maximum upward acceleration is about 50% greater than the maximum downward acceleration, and reaches g for train speeds greater than at least 70 m/s (250 km/h), depending on the track support system stiffness. However, the peak accelerations may not be sufficiently long-lasting to cause enhanced deterioration of the trackbed. This also applies to the higher frequency accelerations from wheel / rail unevenness, which may be of extremely short duration. More work is needed to determine

the thresholds of duration and magnitude at which accelerations begin to damage the trackbed.

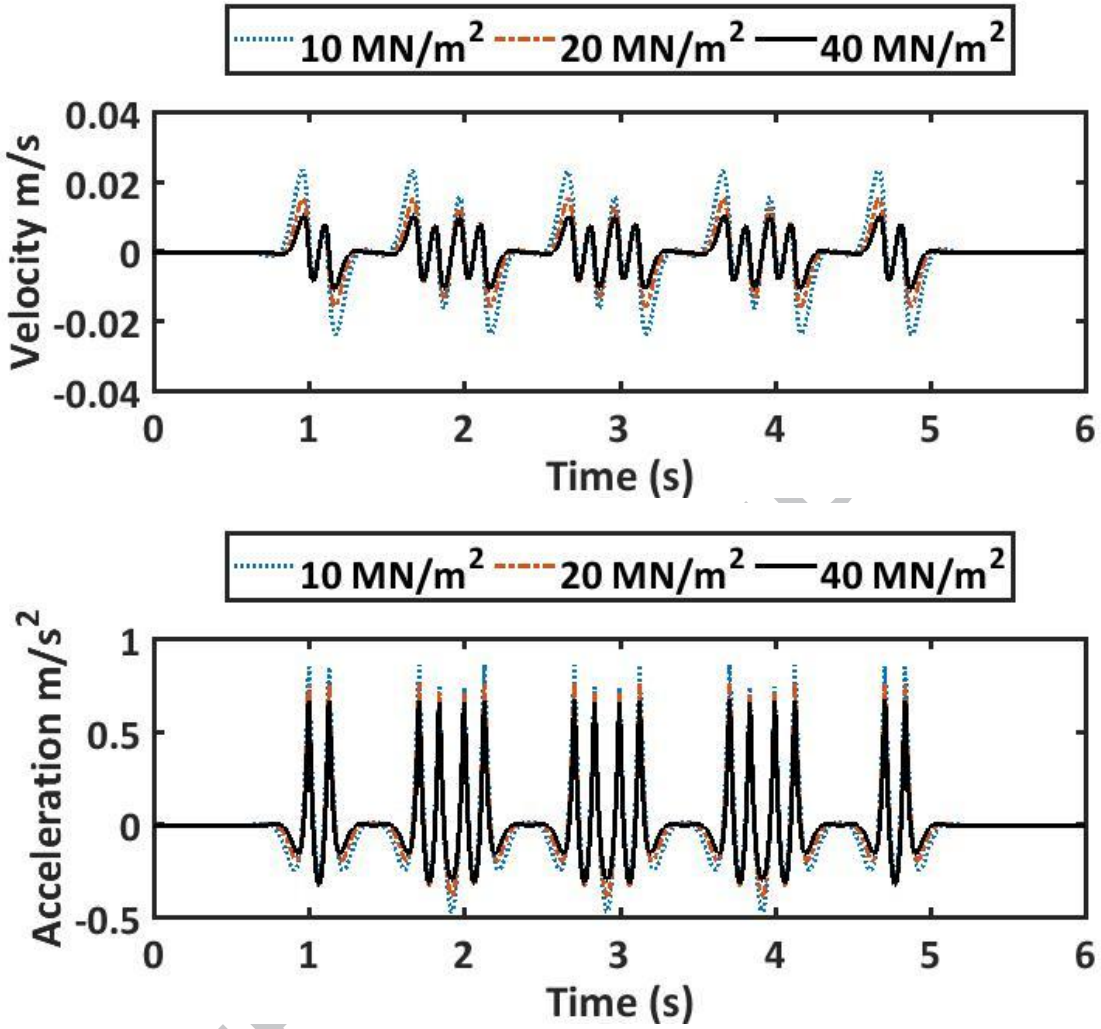

Figure 8: BOEF model (a) velocities and (b) accelerations corresponding to the displacements in Figure 7 for a 20 m/s Javelin train

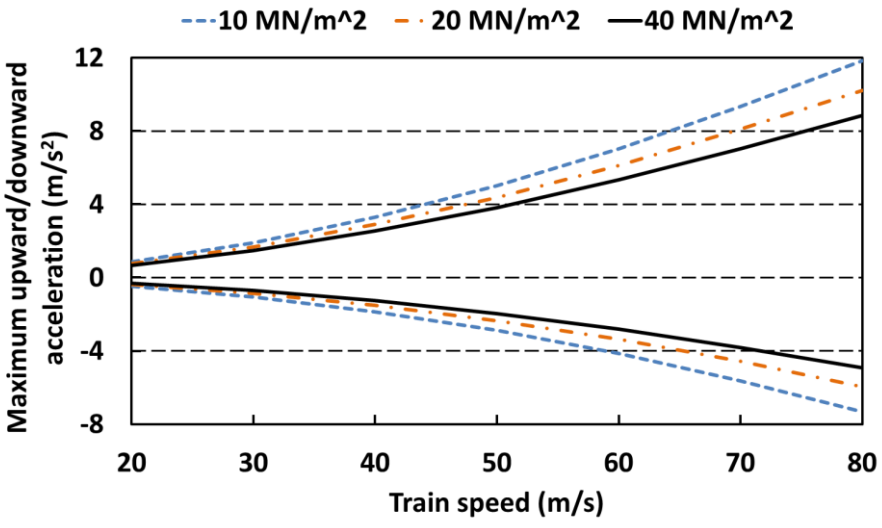

Figure 9: Maximum and minimum accelerations for different train speeds and track support system modulus

Figure 7 and Figure 8 show results from applying Equation (5) in the time domain. Further insight into loading frequency effects may be obtained by considering solutions in the frequency domain, through combining the Fourier transforms in terms of circular frequency ω ($\omega=2\pi f$, for frequency f in Hz) for the shape function in Equation (3)

$$S(\omega) = \frac{1}{2kL}\int_{-\infty}^{\infty} e^{-\frac{v|t|}{L}}\left(\cos\left(\frac{v|t|}{L}\right) + \sin\left(\frac{v|t|}{L}\right)\right)e^{-i\omega t}\,dt = \frac{4v^3}{4kv^4+kL^4\omega^4} \quad (6)$$

and for the load function in Equation (4)

$$P(\omega) = \sum_{n=1}^{N}\int_{-\infty}^{\infty} F_n\,\delta\left(t-\frac{d_n}{v}\right)e^{-i\omega t}\,dt = \sum_{n=1}^{N} F_n e^{-\frac{i\omega d_n}{v}} \quad (7)$$

to give the displacement amplitudes as the Fourier transform of Equation (5)

$$W(\omega) = \frac{4v^3}{4kv^4+kL^4\omega^4}\sum_{n=1}^{N} F_n e^{-\frac{i\omega d_n}{v}} \quad (8)$$

The shape function, $S(\omega)$, in effect scales the amplitudes of the loading spectrum, $P(\omega)$, to give the displacements, $W(\omega)$. For a given rail section, the shape function depends only on the track support system modulus (k) and the train velocity (v).

The velocity and acceleration spectra may be determined by multiplying Equation 8 by $i\omega$ and $-\omega^2$, respectively. Equations 6, 7 and 8 may be applied to any train, having any combination of axle loads and spacings. Figure 10 parts a, c, and e show Equation 6 (the shape function) and its derivatives plotted for a train travelling at a speed of 20 m/s on track with 60 E1 rails. The theoretical spectra for a 4-vehicle Javelin train, formed from the combined shape and load functions, are shown in Figure 10 parts b, d, and f. The shape function results in a rapid attenuation of the amplitude as the frequency increases; even for acceleration, there is proportionally very little content above 20 Hz for a train speed of 20 m/s.

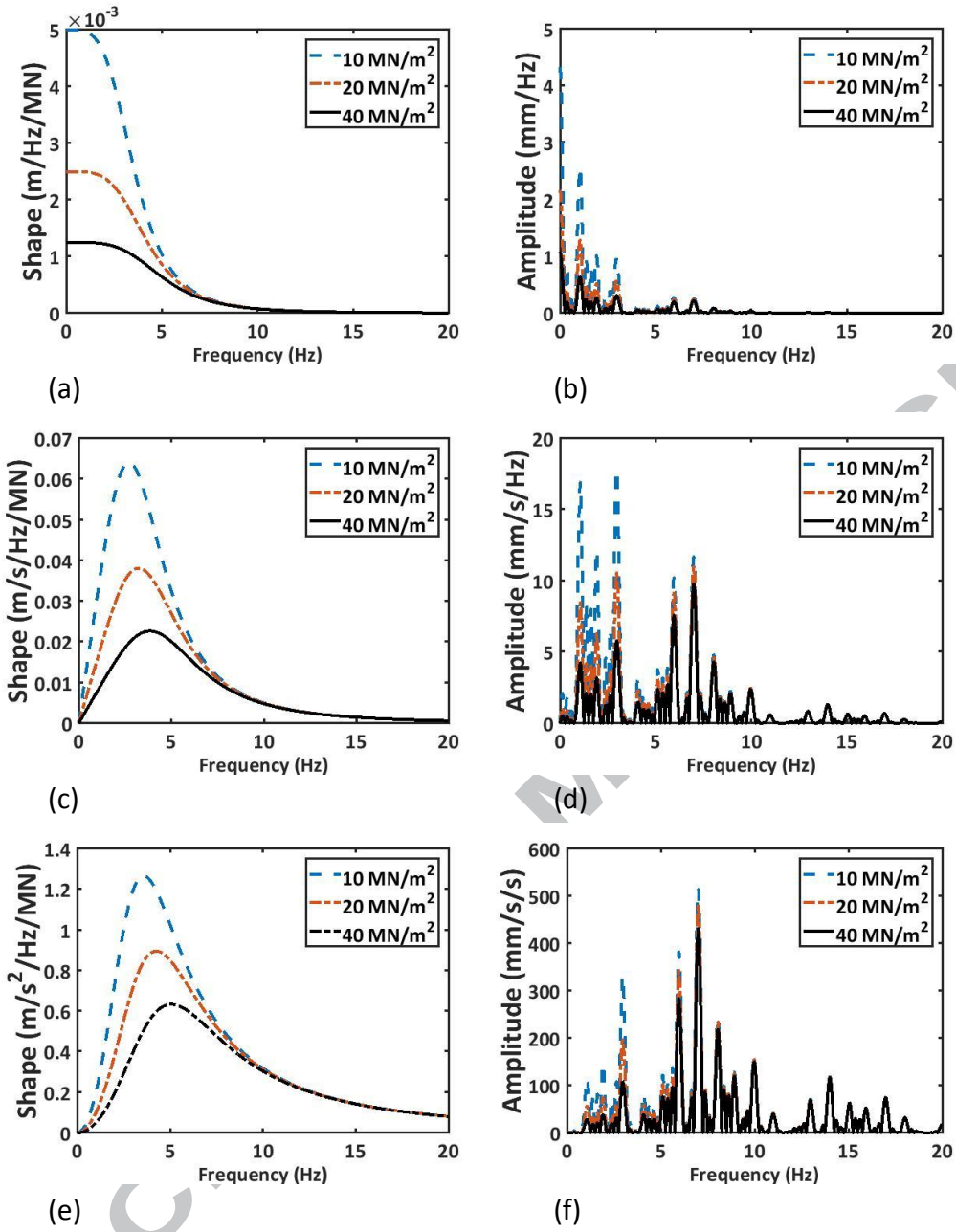

Figure 10: (a, c, e) shape functions and (b, d, f) response spectra for displacement, velocity and acceleration respectively

The velocity spectrum shown in Figure 10(d) is qualitatively similar to measured velocity spectra obtained using geophones for a variety of train geometries (Table 3), reported by Milne et al (2017) and reproduced here in Figure 11. The frequency axis has been normalised by the vehicle passing frequency $f_1=v/L_v$, where L_v is the length of the primary vehicle in the train (i.e., the normalised frequency $N=f/f_1$). The actual magnitudes of velocity (and acceleration) depend on the train speed, but their relative values do not.

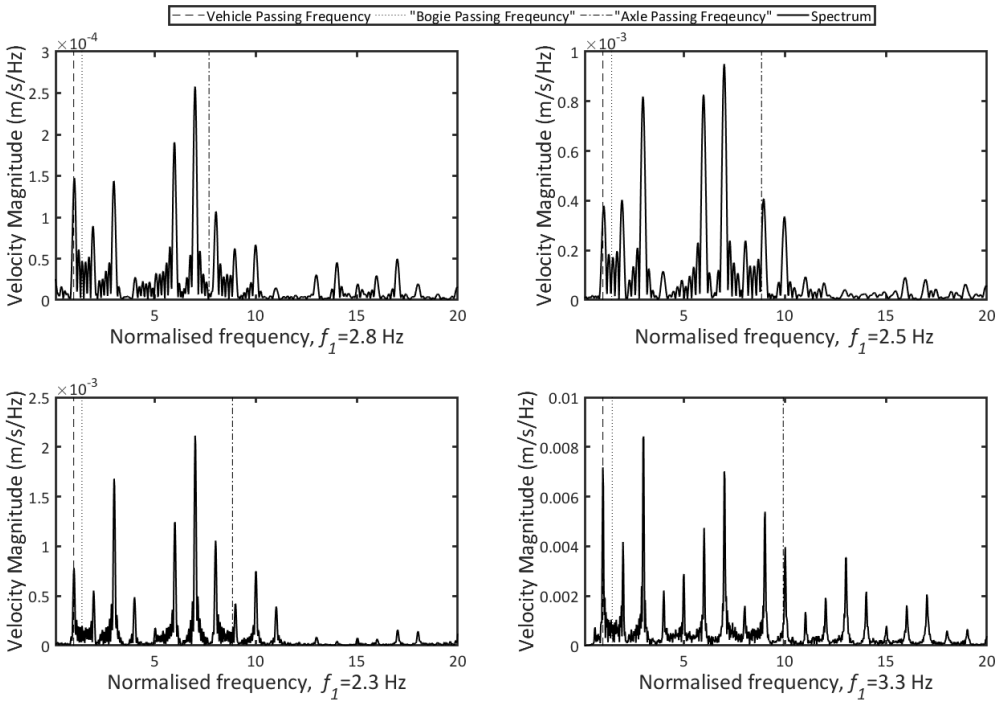

Figure 11: Measured sleeper velocity spectra for a) 6 car Javelin (56.4 m/s); b) 5 car Voyager (56.3 m/s); c) 11 car Pendolino (54.2 m/s); d) 16 car Valero (80.8 m/s) (Milne et al 2017)

Train type	No. of vehicles	Vehicle length L_v, m	Bogie spacing L_b, m	Axle spacing L_w, m
a) Javelin	6	20	14.2	2.6
b) Voyager	5	23	16	2.6
c) Pendolino	11	23.9	17	2.7
d) Valero	16	24.8	17	2.5

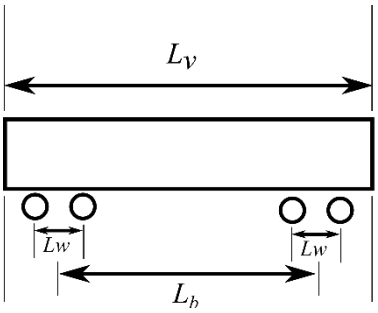

Table 3: Example train geometries (Milne et al 2017)

Figure 11 confirms that the velocity spectra of common train types exhibit prominent peaks at approximately integer multiples of the vehicle passing frequency (as noted by Ju et al 2009). These are the dominant frequencies. Theoretical “bogie” or “axle” frequencies are not dominant. For example, the “axle frequencies” (the axle spacings divided by the train speed) for these four trains are 7.7 Hz, 8.8 Hz, 8.9 Hz and 9.9 Hz respectively, but these do not appear as peaks in the spectra. However, it will be shown that the spacing between pairs of bogies and axles are important in modulating the amplitudes of the dominant frequencies. A further point is that longer trains give narrower peaks.

Equations 6, 7 and 8 were developed for a general train with possibly irregular loads and axle spacings. By considering the special case of a train formed of a single repeating vehicle type, the effect of the number of vehicles in a train on the loading spectrum may be explored. For a single vehicle having four equal axle loads F, an overall length L_v, a distance between bogie centres L_b and a distance between axles on the same bogie L_w, the Fourier transform of the load function (Equation 7) can be expressed in terms of multiples N (= f/f_1) of the vehicle passing frequency as:

$$P(N) = 4\mathrm{N}\, F \cos\left(\frac{\pi N L_b}{L_v}\right) \cos\left(\frac{\pi N L_w}{L_v}\right) \quad (9)$$

The two terms in Equation 9 permit separate consideration of the spectra associated with the bogie spacing (L_b) and the axle spacing (L_w) (Figure 12).

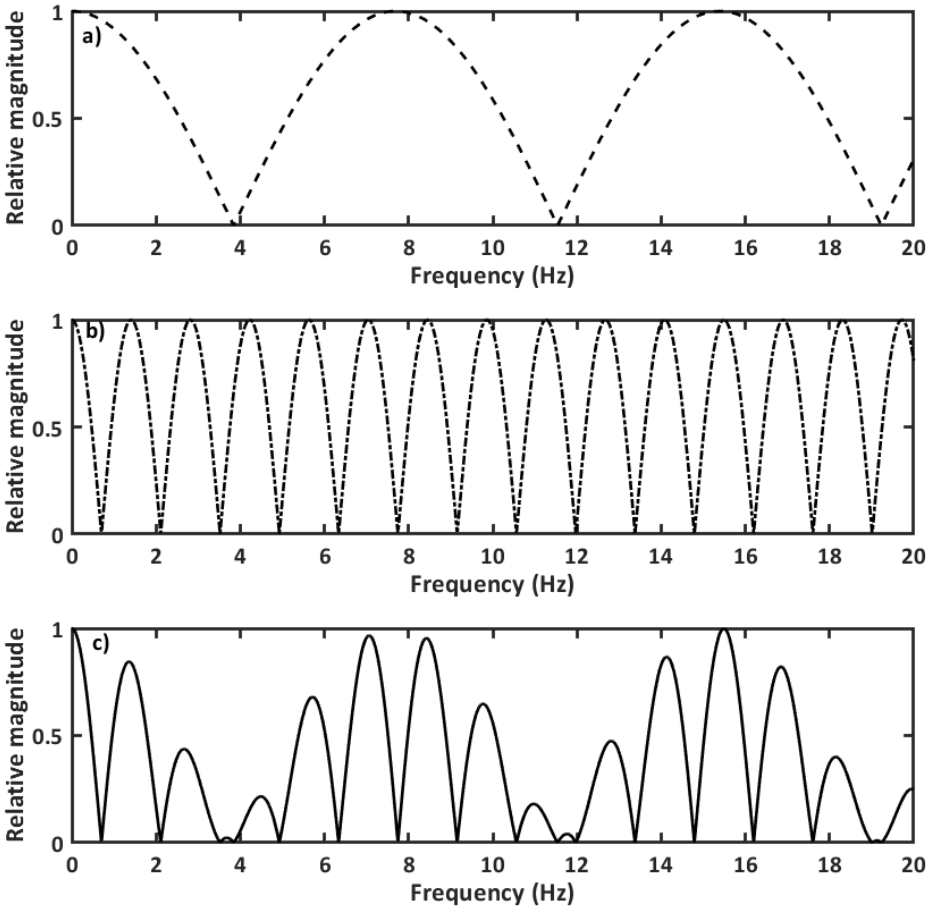

Figure 12 Components of the loading spectrum for a single vehicle; a) contribution of axle spacing - - -; b) contribution of bogie spacing – · –; c) resulting single vehicle spectrum —' for a 20 m long Javelin vehicle at 20 m/s (Milne et al 2017)

The Javelin vehicle has a length of 20 m, a bogie spacing of 14.2 m and an axle spacing of 2.6 m. At a speed of 20 m/s, the vehicle passing frequency is 1 Hz, and frequencies associated

with the axle spacing and the bogie spacing may be calculated as 20/2.6 = 7.7 Hz and 20/14.2 = 1.4 Hz respectively. The spectra for the axle and bogie spacings (Equation 9) are periodic and have local maxima at these frequencies and integer multiples thereof. These are apparent in parts a and b of Figure 12, but in the combined spectrum (Figure 12c) the axle and bogie passing frequencies modulate each other and are no longer individually distinguishable. Passage of a number of similar vehicles provides a further overlay and may be accounted for by the Fourier transform of the load function for a train of N_c vehicles, resulting in an additional series (summation) term as in Equation 10 (Milne et al 2017).

$$\mathrm{P}(N) = NF \cos\left(\frac{\pi N L_b}{L_v}\right) \cos\left(\frac{\pi N L_w}{L_v}\right) \sum_{m=0}^{N_c-1} e^{-i2\pi Nm} \tag{10}$$

Figure 13 shows that increasing the number of vehicles brings the prominent peaks closer to integer multiples of the vehicle passing frequency. Intervening peaks are comparatively small for trains with four or more similar vehicles (Le Pen et al 2016, Milne et al 2017). This means that the axle or bogie passing frequencies are not themselves dominant within the train load or track vibration spectrum, unless the axle spacing happens to be an integer fraction of the vehicle length.

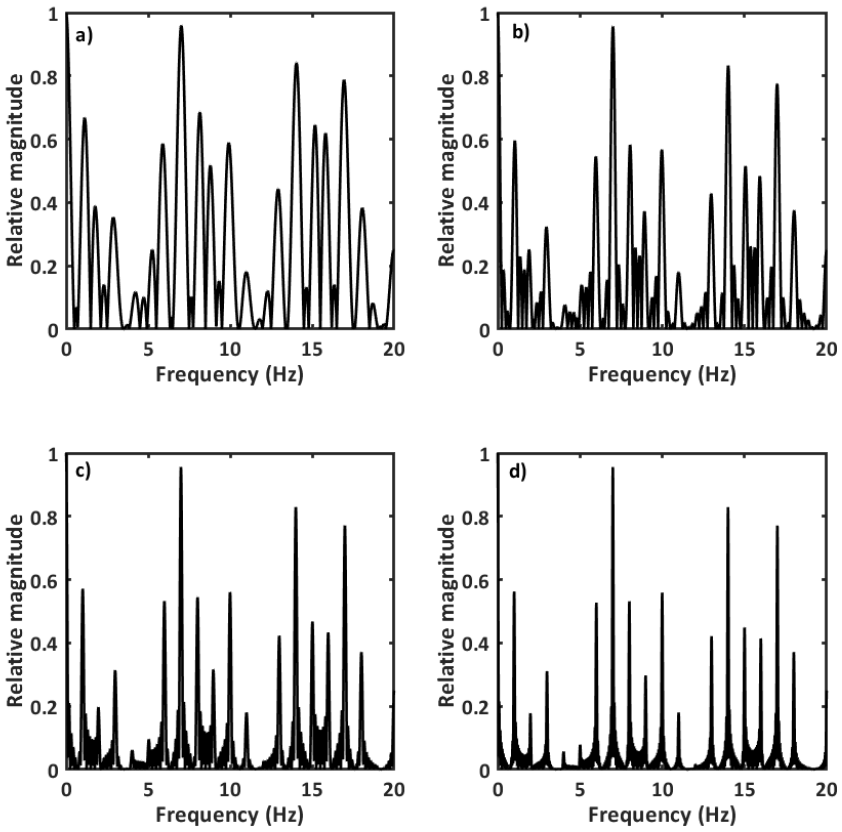

Figure 13 loading spectra a train comprising (a) 2, (b) 4, (c) 8, (d) 16 no. 20 m long Javelin vehicles travelling at 20 m/s (Milne et al 2017)

A train that is (in theory, infinitely) long will be periodic for the repeating vehicle. The train loads, track movements or load per sleeper end may then be treated as a complex Fourier series, with coefficients at multiples of the vehicle passing frequency. This is convenient for studying the effects of train loading in an idealised way, or generating cycles of train loading for testing. In particular, it shows how many integer multiples of the vehicle passing frequency are relevant in terms of their influence on the displacement, velocity and acceleration spectra (Figure 14) for a Javelin train. With the first 20 terms, 99% of the actual maximum displacement is recovered, 102% of the velocity and 76% of the acceleration.

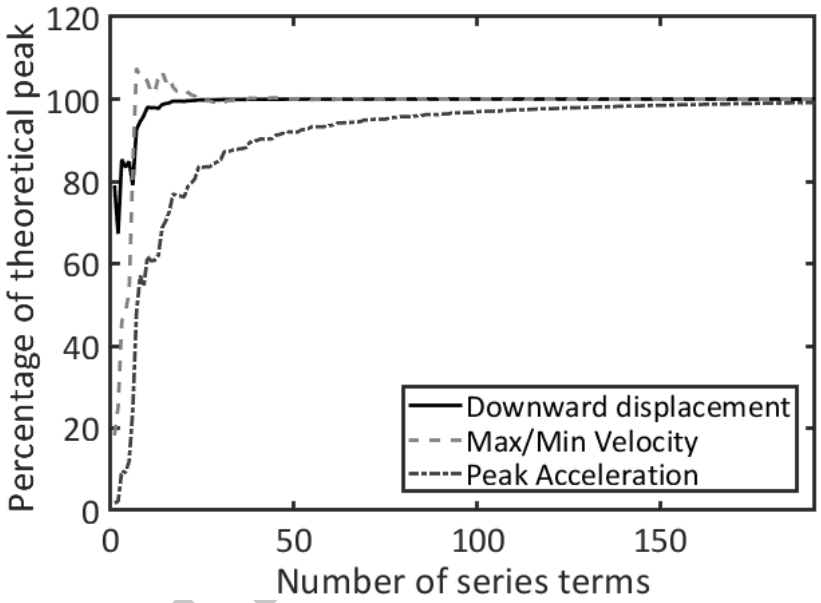

Figure 14: Multiplies of the vehicle passing frequency needed to calculate the actual peak values of displacement, velocity and acceleration: percentage of theoretical peak* vs *number of terms in complex Fourier series

Figure 15 shows the first 20 Fourier coefficients and how they combine to give Fourier series approximations for the deflection, velocity and acceleration spectra for a repeating period of an infinite train.

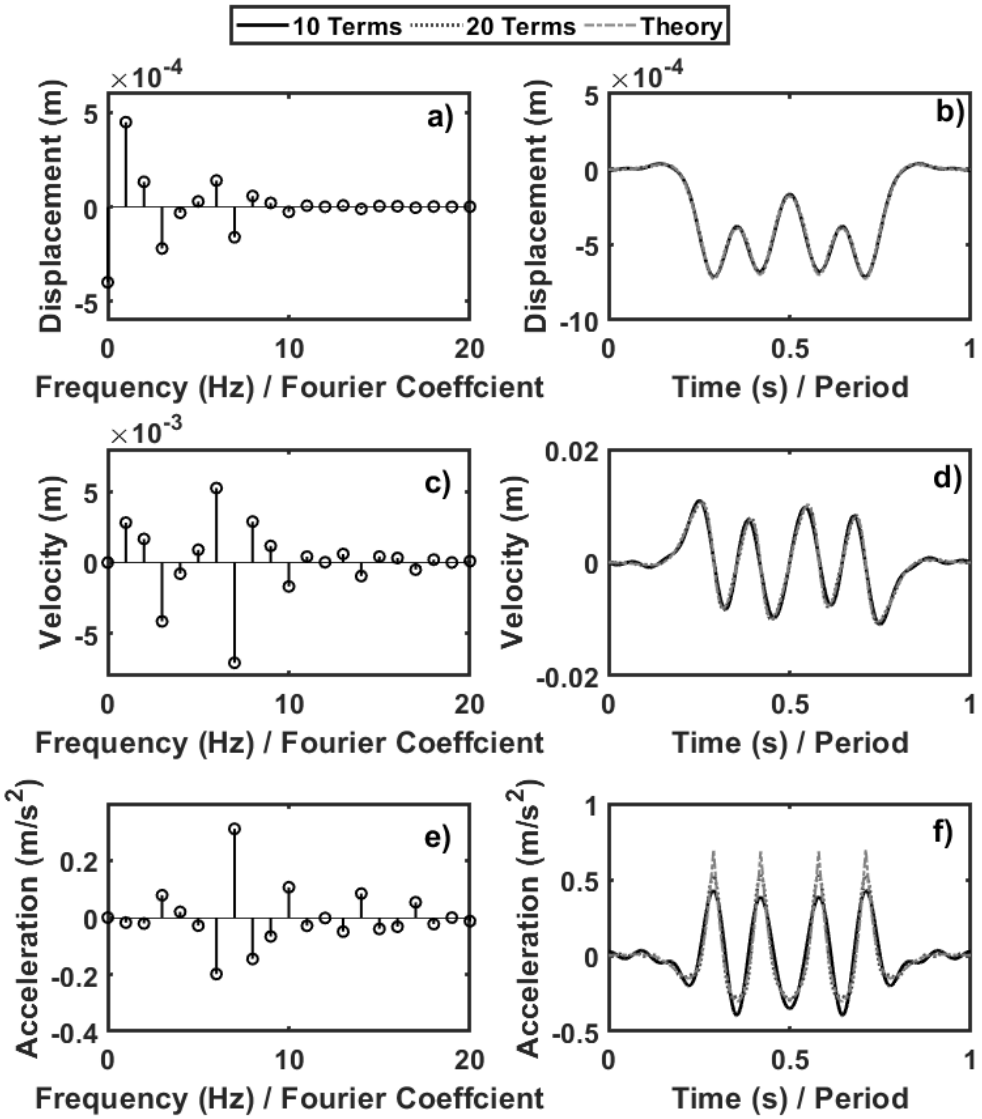

Figure 15: First 20 Fourier coefficients for (a) displacement, (b) velocity, (c) acceleration and Fourier series representation using 20 terms and theory of (d) displacement, (e) velocity, (f) acceleration for a Javelin moving at 20 m/s on a track with a 60E1 rail and support system modulus of 40 MPa

Figure 15 shows how the track movement (and hence the relevant loading) is made up of a combination of different components at multiples of the vehicle passing frequency. An important corollary of this is that increasing the testing frequency in a single-frequency cyclic test to match the shortest wheel spacing in a vehicle while maintaining the same loading amplitude is not representative of train-induced loading. It does not account for the fact that the train loading waveform arises from interactions between adjacent axles, bogies and vehicles. The displacement (hence strain) associated with the passage of a train is dominated by low integer multiples of the vehicle passing frequency, with the relatively low frequencies and small displacements of well performing track leading to generally small velocities and accelerations. Peak accelerations in a single frequency test will also tend to be

higher than from a full train of loads as shown in Table 4 for a Javelin on a track with a 60E1 rail and a system support modulus of 40 MN/m^2 and for single cyclic frequency with the same deflection (0.7 mm) These accelerations are at the level of the track; attenuation by the rail pad will further reduce those experienced by the ballast and the underlying soil.

Table 4. Comparison of peak accelerations from a full train of loads and equal cyclic deflection at a single frequency

Speed (m/s)	Theoretical passing frequency (Hz)			Acceleration from full train (m/s^2)		Peak acceleration from cyclic single frequency (m/s^2)		
	Vehicle	Bogie	Axle	max	min	Vehicle	bogie	Axle
20	1.0	1.4	7.7	0.69	-0.30	0.03	0.06	1.70
40	2.0	2.8	15.4	2.76	-1.22	0.11	0.23	6.80
60	3.0	4.2	23.1	6.20	-2.74	0.26	0.51	15.30
80	4.0	5.6	30.8	11.03	-4.86	0.46	0.91	27.20

Furthermore, the accelerations associated with different frequencies will generally not be in phase; and the application of a load increases the confining stress which, according to the data of Sun et al (2018) summarised in Table 1 increases the acceleration that the ballast can withstand while maintaining its integrity.

ATTENUATION OF LOAD AND FREQUENCY WITH DEPTH

The line load applied by a rail to the ground may be approximated using the BOEF model, $q(x) = w(x)/k$ with $w(x)$ calculated from Equation (5) (assuming continuous rather than discrete support from the sleepers), may be convolved with the Boussinesq solution for the vertical stress σ_v in a homogeneous elastic solid at a depth z, distance along the rail, and horizontal offset from the load a (Poulos and Davis 1973),

$$\sigma_v(x,z) = \frac{3z^3}{2\pi}\int_{-\infty}^{\infty}\frac{q(x)}{\sqrt{(a-x)^2+z^2}^5}\,dx \qquad (11)$$

This may be solved to give contours of vertical effective stress increase in the ground. Those resulting from the pressure applied by four wheel loads of 54 kN at a pair of vehicle ends on a track with a support system modulus of 40 MN/m^2 and a E1 60 rail are shown in Figure 16. The stress reduces with depth below the surface, and the influence of individual wheels and then bogies becomes less pronounced as seen in 3D finite element analyses by, for example, Powrie *et al* (2007).

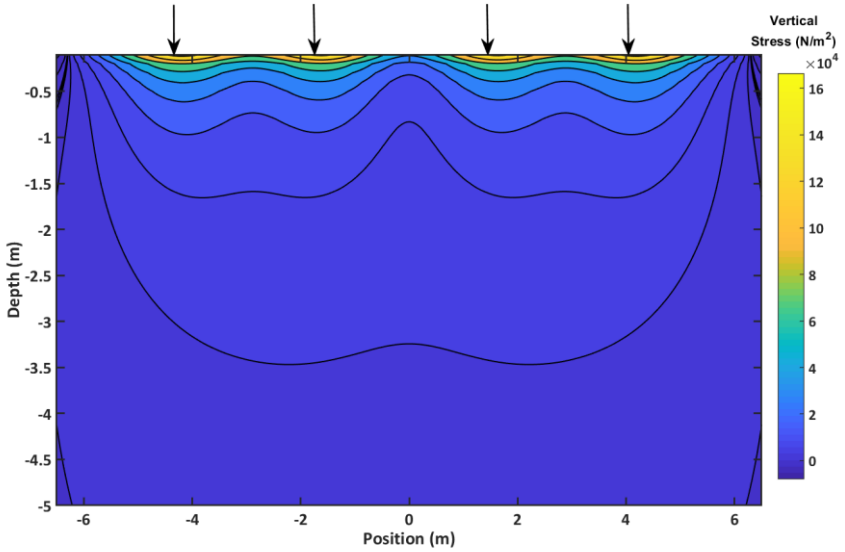

Figure 16: Vertical stress beneath a rail loaded by the ends of two Javelin vehicles

The stress contours in Figure 16 are reflected in the changes in vertical effective stress as a function of time at depths of 0.315 m, 1.186 m and 4.04 m below the sleeper soffit computed in the 3D finite element analyses (Powrie et al 2007) and corroborated by displacements measured using buried geophones (Priest et al 2010; Figure 17. This confirms the significance of the vehicle passing frequency as a basic characteristic of train loading.

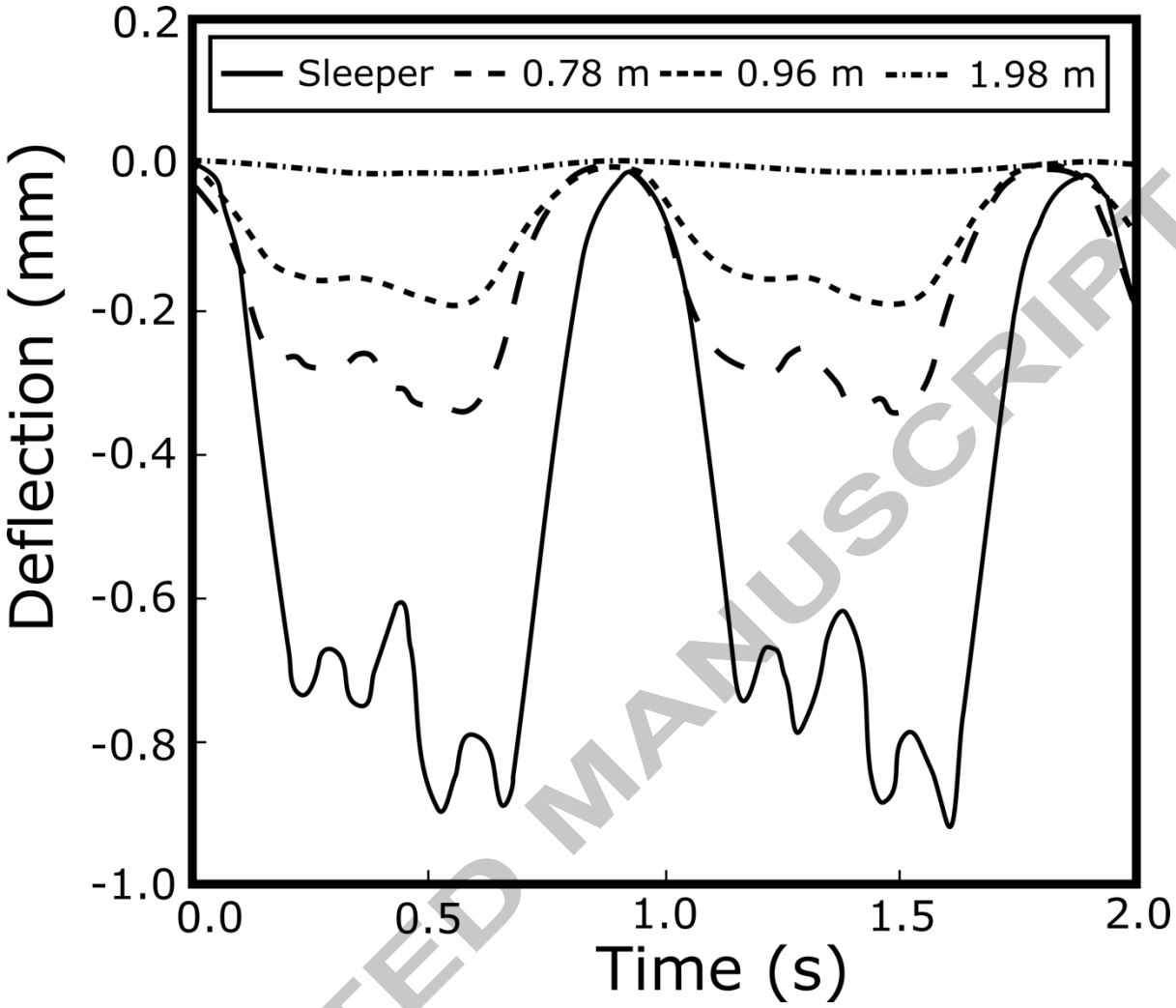

Figure 17: Displacements at depths of 780 mm (Hole A), 955 mm (Hole B), and 1980 mm (Hole C) below the sleeper soffit on a South African heavy haul railway line, measured by Priest et al (2010)

The Fourier transform of the Boussinesq solution for the stresses at different depths beneath a track loaded by a single axle further demonstrates the attenuation of higher frequency components with depth, as illustrated in Figure 18 for a load moving at 20 m/s. The inference of Figures 15 to 17 for soil testing is that, for materials at depth, the higher frequency components of even the quasi-static loading from trains become increasingly less relevant.

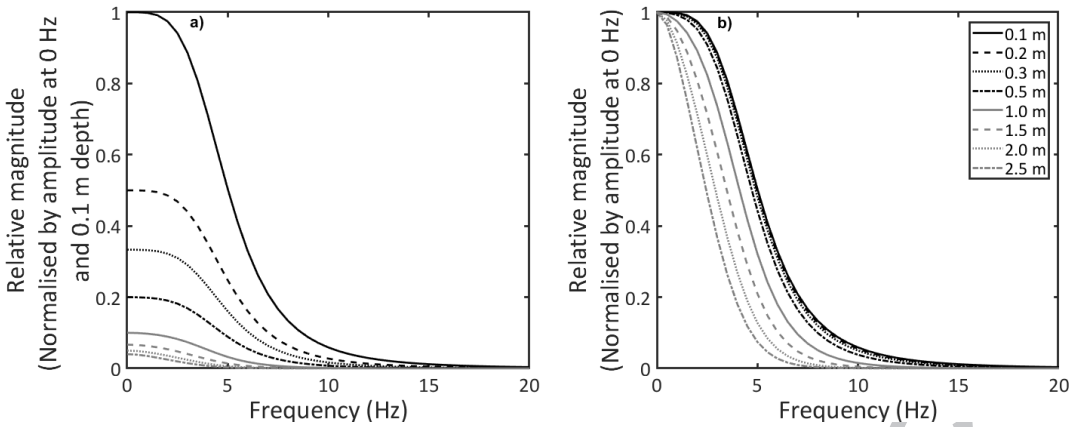

Figure 18: Effect of depth on frequency content for vertical stress beneath a loaded rail (a) highlights the effect on magnitude and (b) the effect on frequency.

CONCLUSIONS

1. Railway loads are generally dynamic, but will usually still elicit a quasi-static response from the materials and structures on which they act. If maximum structure or material accelerations exceed certain magnitude and duration (frequency) thresholds, dynamic response effects may need to be considered. Acceleration depends on both frequency and amplitude of vibration (hence train speed, track stiffness and load).
2. The behaviour of materials under cyclic loading is complex. The principal behavioural regimes may be categorised as shakedown, cyclic creep and ratcheting to collapse. Material deterioration (wear) effects may be significant. Cyclic behaviour of structures such as the ballast bed may also involve geometric effects, e.g. the lateral spread of ballast.
3. Principal stress rotation may be an important consideration at depths between 0.3m and up to at least 2 m below the sleeper soffit.
4. In intermediate permeability soils, the drainage time between episodes of loading characterised by a complete train passage may also need to be considered.
5. Trains exert spectra of loads, with peaks associated with integer multiples of the vehicle passing frequency. The load spectrum experienced by the soil depends on the vehicle speed and the geometry of cars, bogies and axles, and also the track support system stiffness and depth. Spectra can be represented by complex Fourier series, with frequencies up to 20 times the vehicle passing frequency responsible for 99% of the maximum displacement, 102% of the maximum velocity and 76% of the maximum acceleration experienced by the track.
6. Higher frequency load components in the soil tend to decrease magnitude with decreasing track support system modulus and with depth.

ACKNOWLEDGEMENTS

The research was funded by the Engineering and Physical Sciences Research Council (EPSRC) through the programme grant Track to the Future (EP/M025276/1). We acknowledge the help and support of staff from Network Rail and Network Rail High Speed in carrying out aspects of the research reported. Data and supplementary details supporting this study are openly available from the University of Southampton repository at https://doi.org/10.5258/SOTON/xxxxx.

REFERENCES

Abadi T, Le Pen L, Zervos A & Powrie W (2018). Improving the performance of railway tracks through ballast interventions. *Proceedings of the Institution of Mechanical Engineers, Part F: Journal of Rail and Rapid Transit* **232**, 337-355

Abadi T, Le Pen L, Zervos A & Powrie W (2016). A Review and Evaluation of Ballast Settlement Models using Results from the Southampton Railway Testing Facility (SRTF). *Procedia Engineering* **143**, 999-1006

Alves Costa P, Calçada R and Silva Cardoso A (2012). Track–ground vibrations induced by railway traffic: In-situ measurements and validation of a 2.5D FEM-BEM model. Soil Dynamics and Earthquake Engineering 32(1): 111-128

Alves Costa P, Calçada R, Silva Cardoso A and Bodare A (2010). Influence of soil non-linearity on the dynamic response of high-speed railway tracks. Soil Dynamics and Earthquake Engineering 30(4): 221-235

American Railway Engineering Association (AREA) (1996). Manual for railway engineering, volume 1. AREA, Washington D C

Auersch L (2005). The excitation of ground vibration by rail traffic: theory of vehicle–track–soil interaction and measurements on high-speed lines. Journal of Sound and Vibration 284(1–2): 103-132

Brown, S F (1996). Soil mechanics in pavement engineering. *Géotechnique* **46**(3), 383-426

British Railways, 1993. Group Standard: Permissible Track Forces for Railway Vehicles, Issue 1, Revision A, Oct 1993, British Railways Board GM/TT0088, Group Standards, Railway Technical Centre, Derby.

BSI (2010). BS EN 1990:2002+A1:2005, *Eurocode - Basis of structural design*. British Standards Institution, London, UK

Collins I F & Boulbibane M (2000). Geomechanical Analysis of Unbound Pavements Based on Shakedown Theory. *Journal of Geotechnical and Geoenvironmental Engineering* **126**(1), 50–59

Connolly D P, Kouroussis G, Woodward P K, Alves Costa P, Verlinden O and Forde M C (2014). Field testing and analysis of high speed rail vibrations. Soil Dynamics and Earthquake Engineering 67: 102-118

Dieterman H A and Metrikine A (1996). Equivalent stiffness of a half-space interacting with a beam. Critical velocities of a moving load along the beam. European Journal of Mechanics, A/Solids 15(1): 67-90

Dieterman H A and Metrikine A V (1997). Steady-state displacements of a beam on an elastic half-space due to a uniformly moving constant load. European Journal of Mechanics, A/Solids 16(2): 295-306

Lord J A, O'Riordan N J & Phear A G (1999). Design and analysis of railway track formation subgrade for high speed railways. In *Rail technology for the future*. Institution of Civil Engineers, London

Mezher, S. B., Connolly, D. P., Woodward, P. K., Laghrouche, O., Pombo, J. & Costa, P. A. (2016). Railway critical velocity – Analytical prediction and analysis. *Transportation Geotechnics*, 6, 84-96.

Esveld C (2001). *Modern Railway Track*, Zaltbommel, MRT Productions

Gräbe P J and Clayton C R I (2009). Effects of principal stress rotation on permanent deformation in rail track foundations', *Journal of Geotechnical and Geoenvironmental Engineering* **135**(4), 555-565

Grassie S L (2012). Rail irregularities, corrugation and acoustic roughness: characteristics, significance and effects of reprofiling. *Proceedings of the Institution of Mechanical Engineers, Part F: Journal of Rail and Rapid Transit* **226**, 542-557

Indraratna B, Ionescu D & Christie H D (1998). Shear behavior of railway ballast based on large-scale triaxial tests. *Journal of Geotechnical and Geoenvironmental Engineering* **124**, 439

Iwnicki, S. (2006) *Handbook of Railway Vehicle Dynamics*. CRC Press.

Jacob C E (1939). Fluctuations in artesian pressure produced by passing railroad-trains as shown in a well on Long Island, New York. *Transactions of the American Geophysical Union; Reports and Papers (Hydrology)* 1939, 666-674

Jenkins, H.H., Stephenson, J.E. and Clayton, G.A. (1974) 'Effect of track and vehicle parameters on wheel/rail vertical dynamic forces', *Railway Engineering Journal*, 3(2), pp. 2-16.

Ju S-H, Lin H-T & Huang J-Y (2009). Dominant frequencies of train-induced vibrations. *Journal of Sound and Vibration* **319,** 247-259

Krylov V V (1995). Generation of ground vibration by superfast trains. *Applied Acoustics* **44**, 149–164

Krylov V V (1996). Vibrational impact of high-speed trains, I: effect of track dynamics. *J Acoust Soc America* **1005**, 3121–3134

Lackenby J, Indraratna B, McDowell G R & Christie D (2007). Effect of confining pressure on ballast degradation and deformation under cyclic triaxial loading. *Géotechnique* **57**, 527-536

Le Pen L, Milne D, Thompson D and Powrie W (2016) Evaluating railway track support stiffness from trackside measurements in the absence of wheel load data. *Canadian Geotechnical Journal* **53**(7), 1156-1166

Li D & Selig E T (1998). Method for railway track foundation design, II: applications. *ASCE J Geotechnical and Geoenvironmental Engineering* **124**(4), 323-329

Lombaert G, Degrande G, François S & Thompson D J (2015) Ground-borne vibration due to railway traffic: a review of excitation mechanisms, prediction methods and mitigation measures. Paper presented at *Noise and Vibration Mitigation for Rail Transportation Systems*

Madshus C & Kaynia A M (2000). High-speed railway lines on soft ground: dynamic behaviour at critical train speed. *Journal of Sound and Vibration*, **231**(3), 689-701

Mamou A, Priest J A, Clayton C R I & Powrie W (2017). Behaviour of saturated railway track foundation materials during undrained cyclic loading. *Canadian Geotechnical Journal* **55**, 689-697

Mezher S B, Connolly D P, Woodward P K, Laghrouche O, Pombo J & Costa P A (2016). Railway critical velocity – Analytical prediction and analysis. *Transportation Geotechnics*, **6**, 84-96

Milne D R M, Le Pen L M, Thompson DJ and Powrie W (2017) Properties of train load frequencies and their applications. *Journal of Sound and Vibration* **397**, 123-140

Poulos H G and Davis E H (1973) *Elastic solutions for soil and rock mechanics*. Wiley

Powrie W, Yang L A & Clayton C R I (2007). Stress changes in the ground below ballasted railway track during train passage. *Proceedings of the Institution of Mechanical Engineers, Part F: Journal of Rail and Rapid Transit* **221**, 247-261

Priest J A & Powrie W (2009). Determination of dynamic track modulus from measurement of track velocity during train passage. *J ASCE Geotechnical and Geoenvironmental Engineering* **135**(11), 1732-1740

Priest J A, Powrie W, Yang L, Grabe P J & Clayton C R I (2010). Measurements of transient ground movements below a ballasted railway line. *Géotechnique* **60,** 667-677.

Qian J-G, Wang Y-G, Yin Z-Y, Huang M-S, (2016). Experimental identification of plastic shakedown behavior of saturated clay subjected to traffic loading with principal stress rotation. *Engineering Geology* **214**, 29–42. Available at: http://dx.doi.org/10.1016/j.enggeo.2016.09.012

Raymond G P (1985). Analysis of track support and determination of track modulus. *Transportation Research Record* **1022**, 80-90

Sato, Y (1995). Japanese studies on deterioration of ballasted track. *Vehicle System Dynamics* **24**, 197-208

Sheng X, Jones CJC and Thompson DJ (2003) A comparison of a theoretical model for quasi-statically and dynamically induced environmental vibration from trains with measurements. Journal of Sound and Vibration 267(3): 621-635

Shenton, M J (1984). Ballast deformation and track deterioration. *Track Technology*. Proceedings of a conference organized by the Institution of Civil Engineers, 253-265. University of Nottingham, UK

Shih JY, Thompson DJ and Zervos A (2017) The influence of soil nonlinear properties on the track/ground vibration induced by trains running on soft ground. Transportation Geotechnics 11: 1-16

Sun Q, Indraratna B & Ngo N T (Published online 2018). Effect of increase in load and frequency on the resilience of railway ballast. *Géotechnique*, 0, 1-8. https://doi.org/10.1680/jgeot.17.P.302

Thompson D (2009). *Railway noise and vibration: mechanisms, modelling and means of control*. Elsevier: Oxford

Timoshenko S (1927). Method of analysis of statical and dynamical stresses in rails. In *Proceedings of the Second International Congress of Applied Mechanics*, 407-420. Zurich, Switzerland. Editor E Meissner. Orell Füssli Verlag, Zürich und Leipzig

Timoshenko S & Langer BF (1932) Stresses in railroad track. ASME Transactions 54: 277-293

Triepaischajonsak N, Thompson D J, Jones C J C, Ryue J & Priest J A (2011). Ground vibration from trains: experimental parameter characterization and validation of a numerical model. *Proceedings of the Institution of Mechanical Engineers, Part F: Journal of Rail and Rapid Transit* **225**, 140-153

Van Dyk B J, Edwards J R, Dersch M S, Ruppert Jr C J & Barkan C P L (2017) Evaluation of dynamic and impact wheel load factors and their application in design processes, *Proceedings of the Institution of Mechanical Engineers, Part F: Journal of Rail and Rapid Transit*, **231**(1), 33-43.

Woldringh R F & New B M (1999). Embankment design for high speed trains on soft soils. In *Geotechnical engineering for transportation infrastructure*, edited by F Barends et al, 1703-1712. AA Balkema, Rotterdam

Yang L A, Powrie W & Priest J A (2009). Dynamic stress analysis of a ballasted railway track bed during train passage. *Journal of Geotechnical and Geoenvironmental Engineering* **135**(5): 680-689